International Journal of Engineering & Technology, 7 (4.35) (2018) 436-441

SPC

International Journal of Engineering & Technology

Website: www.sciencepubco.com/index.php/IJET

Research paper



Applications of Landsat-8 Data: a Survey

M. A. Ridwan[1]*, N. A. M. Radzi[2], W. S. H. M. W. Ahmad[3], I. S. Mustafa[4], N. M. Din[5], Y. E. Jalil[6], A. M. Isa[7], N. S. Othman[8], W. M. D. W. Zaki[9]

[1]Electronics Research Group, Dept. of Electronics and Communication Engineering,
College of Engineering, Universiti Tenaga Nasional,
Jalan Ikram-Uniten, 43000 Kajang, Malaysia
[2]Center for Integrated Systems Engineering & Advanced Technologies (INTEGRA),
Faculty of Engineering and Built Environment,
Universiti Kebangsaan Malaysia, 43600 UKM Bangi, Selangor DE, Malaysia
**Corresponding author E-mail: m.azmiridwan@gmail.com*

Abstract

Landsat 8 was launched in 2013 by the National Aeronautics and Space Administration (NASA). On board of the Landsat 8 is the Operational Land Imager (OLI) and Thermal Infrared Sensor (TIRS). Data for visible, panchromatic band, short-wave infrared spectral bands are collected by the OLI while TIRS collect images in the thermal region. As data for Landsat 8 is available to be used for public, researchers have utilized the data for numerous applications. However, to the best of our knowledge, there is yet a review paper on the various applications of Landsat 8 data. Hence, this paper presented an innovative survey on Landsat 8 data in the application of agriculture and forestry, land use and mapping, geology, hydrology, coastal resources and environmental monitoring. The potential of utilizing Landsat 8 data for power utility companies is also discussed in this paper. As Landsat 8 data is predicted to be available for more years to come, this paper provides insight for researchers to utilize the data better for their research.

Keywords: *Landsat 8; remote sensing; review; survey; power related.*

1. Introduction

Launched in July 1972, Earth Resources Technology Satellite (ERTS-1) or later renamed as Landsat 1 is the first civilian Earth observation satellite in the world. On board of the Landsat 8 is the Operational Land Imager (OLI) and Thermal Infrared Sensor (TIRS). Data for visible, panchromatic band, short-wave infrared spectral bands are collected by the OLI while TIRS collect images in the thermal region.

With the success achieved by the Landsat 1, more Landsats are launched by the U. S. Geological (USGS) and National Aeronautics and Space Administration (NASA) including the Landsat 2 (1975), Landsat 3 (1978), Landsat 4 (1982) and Landsat 5 (1984). The failure of Landsat 6 to achieve its orbit in 1993 has been a setback to researchers considering Landsat 5 has set a Guinness World Record for "longest-operating Earth observation satellite" as it has been operating for 28 years and 10 months. USGS/NASA bounced back with Landsat 7 that has been launched in 1999 and the most recent satellite launched is Landsat 8 in 2013. Landsat 9 is planned to be launched in 2020 with a timeline depicted in Figure 1.

2. Background Study

Landsat 8 has a solar synchronization orbit with a nominal spacecraft altitude of 705 km with the ability to orbit the earth every 98.9 minutes. 400 scenes are captured by the Landsat 8 and it is downlink to the USGS data archives. The scenes acquired by Landsat 8 is 185 km cross track by 180 km along track with regression cycle of 16 days. The design life of the Landsat 8 is 5 years and has 10 years of fuel carried onboard. For commanding and housekeeping telemetry operations, S-Band is used whereas for instrument data downlink, X-band is used.

Landsat 8 Ground Stations are situated in these five locations; 1) Landsat Ground Station in South Dakota, 2) Svalbard Ground Station in Norway, 3) Alice Springs Ground Station in Australia, 4) Neustrelitz ground station in Germany and 5) Gilmore Creek ground station in Alaska. The functions of the ground system are to command and control the Landsat 8 observatory in orbit as well as to manage the data transmitted from the observatory.

Landsat 8 was launched from Vandenberg Air Force Base, California, on an Atlas-V 401 rocket. It carried onboard two sensors; Operational Land Imager (OLI) and Thermal Infrared Sensor (TIRS) as opposed from prior Landsat where the thermal and reflective band images were acquired with the same sensor. OLI is a sensor equipped with a four-mirror telescope and a quantization of 12 bits. It has the ability to collects data for various spectrum including visible (VIS), near infrared (NIR), short wave infrared (SWIR) bands and a panchromatic band at 0.4-2.5 µm spectrum. On the other hand, TIRS collect images in the thermal region at 10–12.5 µm spectrum. The specifications of OLI/TIRS is shown in Table 1.

Coastal/aerosol, Band 1 senses deep blues and violets where it is used to image shallow water and track fine particles such as dust and smoke. The output of Band 1 is similar to Band 2; however, the differences can be observed by contrasting and highlighting areas with more deep blue. With the request for higher resolution for ocean color investigations, Band 1 was equipped in Landsat 8 [2]. Bands 2, 3, and 4 are visible blue, green, and red.

Copyright © 2018 Authors. This is an open access article distributed under the Creative Commons Attribution License, which permits unrestricted use, distribution, and reproduction in any medium, provided the original work is properly cited.

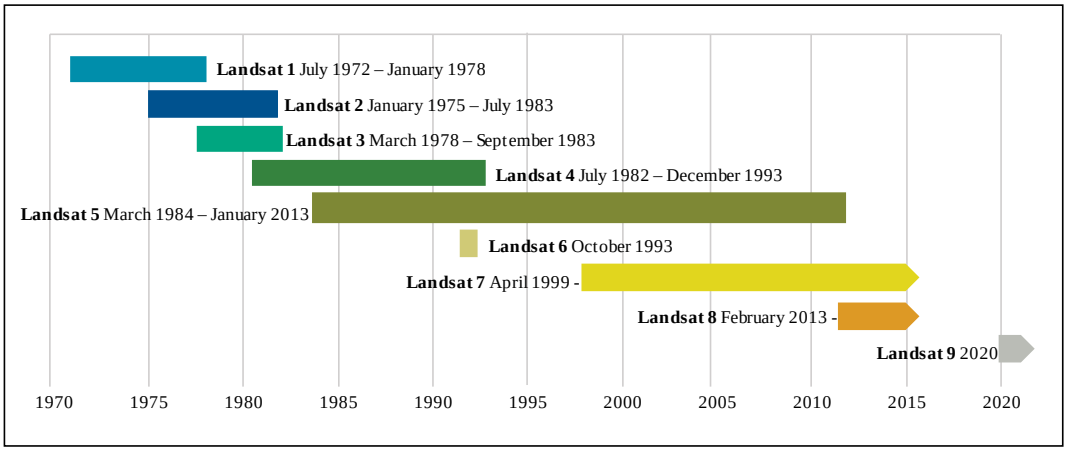


Fig. 1: Timeline and History of Landsat Mission (adapted from [1]).

Table 1: Specifications of OLI/TIRS

Sensor	Band Number	Band	Wavelength (μm)	Resolution
OLI	1	Coastal/ Aerosol	0.435 - 0.451	30m
	2	Blue	0.452 – 0.512	
	3	Green	0.533 – 0.590	
	4	Red	0.636 – 0.673	
	5	Near Infrared	0.851 – 0.879	
	6	SWIR 1	1.566 – 1.651	
	7	SWIR 2	2.107 – 2.294	
	8	Panchromatic	0.503 – 0.676	15m
	9	Cirrus	1.363 – 1.384	30m
TIRS	10	TIRS 1	10.6 – 11.19	100m
	11	TIRS 2	11.50– 12.51	

NIR, Band 5 is a spectroscopic method that uses the near-infrared region of the electromagnetic spectrum is used to obtain normalized difference vegetation index (NDVI), which is a crude estimation of vegetation health and a means of monitoring changes in vegetation over time. Healthy vegetation reflects very well in the NIR part of the spectrum. NDVI is achieved by using two bands; VIS band and NIR band by using Equation 1.

$$NDVI = \frac{NIR - VIS}{NIR + VIS} \quad (1)$$

SWIR is covered in both Band 6 and Band 7 to differentiate wet earth and dry earth as well as rocks and soil. On the other hand, panchromatic is covered in Band 8 where it collects visible colors separately and combine them into one channel, making it black and white. With a resolution of 15 m, panchromatic is the sharpest of all bands. Hence, by combining high resolution panchromatic with lower resolution multispectral imagery in a process called pan sharpening will produce a single high resolution colour image. The changes done in Landsat 8 compared to Landsat 7 is that at Band 4 – 8, bandwidth refinements are made to avoid atmospheric absorption features.

Band 9 covers a thin slice of wavelengths; 1370 ± 10 nanometers. Atmosphere absorbs almost this entire spectrum; however, Landsat 8 turns this into an advantage by using it to capture clouds especially Cirrus cloud. This band is added only in Landsat 8 to detect Cirrus contamination in other channels.

Bands 10 and 11 are TIR band where they sense heat on the ground. Band 10 is usually used to estimate surface brightness temperature in conjunction with an atmospheric model. However, Band 11 as according to notice from USGS, Jan. 6, 2014, has high ambiguity in calibration, hence it is suggested to refrain from relying on this band. These two bands are also newly addition bands in Landsat 8.

Level 1 Landsat 8 archive data is open for public and can be downloaded for free from USGS's Earth Explorer website and bulk downloading are supported from Global Visulization Viewer or LandsatLook Viewer websites. Level 2 data can also be downloaded from EarthExplorer or EROS Science Processing Architecture (ESPA) on-demand interface websites.

The data has been used widely by researchers in numerous applications such as agriculture, forestry, and land use. However, to the best of our knowledge, there is yet a review paper on Landsat 8 applications. Hence, this paper discusses for the first time a survey on Landsat 8 data applications. The rest of the paper is organized as follows; Section II surveys related work, Section III provides the possibility of using the data for power utility companies and Section IV delivers the conclusion of the paper.

3. Application of Landsat 8

Landsat was earlier used especially for remote sensing, however, it has evolved in more diverse field such as agriculture, forestry and range resources, land use and mapping, geology, hydrology, coastal resources and environmental monitoring in these recent years. This paper reviews the researches that have been done for each application mentioned.

3.1 Agriculture and Forestry

Landsat 8 is able to perform swift, accurate and frequent inventories in terms of agriculture. In Gokceada, Turkey, Kadafar and Genc [3] combine Landsat 8 OLI images with Geographic Information Systems (GIS) to find suitable lands for agriculture and to assess their suitability levels. The first 7 OLI bands for two different months; July 2013 and August 2013 together with the 14-band combination image were processed using Erdas Imagine software, which later are used to identify land use land cover maps including six main classes ("Forest", "Agriculture", "Water Surface", "Residential Area-Bare Soil", "Reforestation" and "Other"). The maps combined with digital elevation model (DEM)-derived slope map and soil maps were used to produce potential agricultural land determination and suitability evaluation by analyzing "Other" class under the assumption it may be used for agricultural purposes in future. This study found out that 902-hectare area is suitable to be used for upcoming agriculture area in Gokceada.

Landsat 8 has also been used by Hasituya et al. to monitor plastic-mulched farmland [4]. Plastic mulch is widely used all over the world, especially in China to suppress weeds and conserve water in crops, fruits and vegetables production. The largest plastic-mulched farmland is in China with a coverage of 25 million hectare in 2013. With that, monitoring the plastic-mulched farmland in China is very crucial due to the imbalance between land surfaces, atmosphere and soil caused by changing of energy, water and

carbon. Besides, environmental pollution is also of a concern as the residues of the plastic are gathered over the years of use, degrading the quality of soil and hence the crops production. Concentrated in Jhizou, China, Landsat-8 OLI imagery of Band 1 - 7 are used to classify the land cover into five classes namely "Plastic-mulched farmland", "Impervious surface", "Vegetation cover", "Water body", and "Bare soil". Plastic-mulched farmland is identified as it has the same spectrum curve shape as soil but with a higher reflectance than other classes on SWIR bands. A new scheme is proposed in [4] which integrates spectral and textual features that is able to monitor the plastic-mulched farmland and at the same time evaluating the performance of Support Vector Machine algorithm using OLI, Google Earth imagery and ancillary data.

A comparison of images captured from Landsat 8 data and unmanned aerial vehicle (UAV) eBee data has also been done by Kavvadias et al. [5] particularly for precision agriculture. Precision agriculture or also known as satellite farming is when information and technology are used to manage farming by observing crops, soils, pests etc. remotely. Band 4 (red) and Band 5 (NIR) are used to generate NDVI to estimate plant health condition, photosynthetic activity and nutrients' scarcity. Band 8 (panchromatic) image is also being used for pan sharpening process. On the other hand, UAV uses 11 cm/pixel for image resolution to produce orthomosaic, reflectance map and NDVI map. By comparing the NDVI values of these two methods, this paper proves that images captured via UAV are agreeable and validated with the Landsat 8 data, proven its suitability to be used in precision agriculture.

Aside from agriculture, Landsat is also an important tool for environmental research and natural resource management. In Burkina Faso Woodland, Karlson et al. [6] maps the tree canopy cover (TCC) and aboveground biomass (AGB) using data acquired by Landsat 8. The study is essential as there are contradicting research findings on the woodlands, some researchers claimed that the tree density have decreased due to land use and climate change whereas other researchers claimed that it has improved due to rainfall and natural regeneration. Field data and WorldView-2 imagery was collected and used as a reference dataset during the first study. Afterwards, three predictor variables are identified from the Landsat 8 data; spectral, texture and phenology variables. For spectral, it collects the value of the top of the atmosphere reflectance, multispectral bands and panchromatic band from Bands 2-8, tasseled cap components and vegetation indices. The texture is calculated by using gray level co-occurrence matrix approach, while phenology is a dry season for time series of NDVI. Based on the variables, Random Forest modeling of TCC and AGB is done, proving that the method is not only suitable, but also simple to be implemented in Burkina Faso woodland. The study conducted in [6] concluded that mapping the TCC is more suitable via Landsat 8 as compared to AGB.

In Croatia, Milas et al. [7] uses Landsat 8 OLI images to assess forest damage using NDVI difference approach. Fast line-of-sight atmospheric analysis of hypercubes (FLASSH) is used to radiometrically and atmospherically correcting the Level 1T images from Landsat 8 data from August 2013 and July 2014. NDVI for each image is then calculated and ENVI software is used to detect the forest damage based on NDVI difference. This obtained results show that the proposed NDVI approach is able to detect any forest changes very well.

GRASS GIS and Quantum GIS open source software is used in Indonesia by Ramdani et al. [8] to provide an inexpensive approach to assess the mangroves forest. Band 1 – 8 of OLI Landsat 8 data were used in [8] where deep blue costal band is used to highlight mangroves and separating them from water bodies, NIR and Red is used to calculate NDVI and NIR and SWIR is used to calculate NDWI. The top-of-atmospheric is converted from the Landsat 8 imagery's digital number by first converting the digital numbers values into radiance values, and then further converts them into reflectance values. Landsat 8 OLI is proven to be suitable for assessment of mangrove forest based on this study.

3.2 Land Use and Mapping

Other than agriculture and forestry, Landsat 8 data has played an important key element in monitoring the changes of land cover and land use as well as for mapping. For an instance, in Beijing, China, Hu et al. [9] have used Landsat 8 data to identify high resolution urban land use maps. Since Landsat 8 provides medium-resolution satellite images that makes it hard to allow the extraction of socioeconomic features, high resolution maps are obtained in [9] by combining the remotely sensed data with open social media data that contains spatiotemporal patterns of human activities. Hence, Landsat 8 OLI images are combined with data on the road networks obtained from Open Street Map (OSM) as well as Point of Interests (POI) data; which is data provided voluntarily by individuals for monitoring users' positions in spatial tracking or geo-caching systems. The map produced by Hu et al. has revealed more spatial pattern details of land use compared to the map released by the government.

A mapping of urban built up areas using normalized difference built-up index (NDBI) of Landsat 8 data has been done in Lahore, Pakistan by Bhatti and Tripathi [10]. This study requires OLI bands 2 – 7, panchromatic band 8 as well as thermal band 10 and 11. NDBI is achieved using Equation 2:

$$\text{NDBI} = \frac{\text{Band 5} - \text{Band 4}}{\text{Band 5} + \text{Band 4}} \quad (2)$$

Where if NDBI is larger than 0; $NDBI_B = 255$, otherwise $NDBI_B = 0$. The same concept applies to NDVI. With that in mind, Equation 3 is used to extract the built-up areas:

$$BU_B = NDBI_B - NDVI_B \quad (3)$$

Equation 3 has later been modified to Equation 4 using continuous NDBI and NDVI:

$$BU = NDBI - NDVI \quad (4)$$

Comparing both build up (Equation 2) and modified build up (Equation 3), Bhatti and Tripathi conclude that modified NDBI approach's performance decreased when applied to Landsat-8 OLI data. Hence, a new method, Built-up Area Extraction Method is proposed in this study to extract built up areas.

Grassland productivity estimation Moderate Resolution Imaging Spectroradiometer (MODIS)-Landsat growing season integrated NDVI (GSN) map has also been done by Gu and Wylie [11] for Central Nebraska using a combination of MODIS GSN and Landsat 8 data. Bands 2 – 7 Landsat 8 data for vegetation mapping together with band 9 for cloud detection are being used in this study. It is concluded that Landsat 8 data can successfully predict the GSN and it was supported by Soil Survey Geographic biomass production map.

Meng and Cheng [12] have done a thorough evaluation on eight global reanalysis products which are commonly used in the atmospheric correction of Landsat 8 TIRS10 data by referencing global radiosonde observations collected from 163 stations. Parameters such as top-of-atmosphere radiances, ability to retrieve land surface temperature (LST), water vapor contents and atmospheric parameters which consist of atmosphere transmittance, upward and downward radiance are tested. The evaluations recommended two of the products namely MERRA-6 and ERA-Interim, for atmospheric corrections of the thermal infrared channel under different surface elevations and water vapor contents.

3.3 Geology

Multispectral data is able to provide information on lithology or rock composition based on spectral reflectance. Due to this reason, Landsat 8 data has also been used for geology. In Plateau state

north central Nigeria, Amusuk et al. [13] has utilized the Landsat 8 imagery data for lithology's map. Differentiation of rock types is done by creating color composite images in this study. NIR is used in performing vegetation analysis, Bands 7, 5 and 3 for rocky outliers, combination of bands 5, 6 and 4 for structural features and Band 3 is to differentiate between wet and dry earth. Any changes in the soil and rocks are able to be detect by SWIR easily, allowing the differentiation of basic type of rocks. Combined with the fact that Landsat 8 is the first series of Landsat with Global Positioning System (GPS), accurate positioning is obtained and in [13] showed that Landsat 8 image data is perfect for the regional and early exploration studies.

In Red Sea State, Zeinelabdein and Nadi [14] have used Landsat 8 data to outline the gossanic ridges to represent prospective targets for gold mineralization. Gossan has a unique characteristic in which it has higher iron oxides compared to the rest of country rocks. Due to this, band rationing technique is used as it is able to accurately map the gossanic ridges. By assigning the ratios OLI 6/7, 4/2, 5/4 to RGB guns, gossans appear in unique colors ranging from reddish orange to red colors with no other rock type shares the color. The outline of these ridges was then done by using on-screen digitizing process. For proof of concept, the ore samples from the delineated gossanic ridges are analyzed via x-ray fluorescence technique and it validates the study done with gold nuggets being collected in the outlined area.

A comparison between Landsat 8 imagery with Landsat 7 imagery has been done by He et al. [15] to study the ability of Landsat 8 in improving the classification results of Landsat 7**.** Using Victoria Island, Canada as its study area, the conventional maximum Likelihood Classifier is compared with recent classifiers: Neural Network, Support Vector Machine and Random Forest, for the purpose of mapping different lithologies. The Natkusiak Formation basalt, Franklin diabase, carbonate of the Wynniatt Formation and the Cambro–Ordovician succession, Palaeozoic dolostones, quartz-arenite of the Kuujjua Formation, and evaporate rocks of the Minto Inlet and Killian formations are the six main lithological units that were defined in this study. NIR and SWIR bands are mainly used for the classifications, followed by visible bands. As expected, the results prove that advanced classifiers performed better than the conventional classifier for Landsat 8 and that Landsat 8 has better performance than Landsat 7, although only slightly. With this, He et al. concluded that Landsat 8 is suitable to be used for geological studies for the next ten years.

Recent work by Abdelaziz et al. [16] discriminates serpentine of the Logar Massif Province in Afghanistan using Landsat 8 OLI data for chromite prospecting. The combination of bands, principal components, band ratios and supervised classification techniques are used to separate the serpentine which is the host of the chromite. Based on the Landsat 8 and maximum likelihood supervised classification as a tool for mineral exploration, the lithological mapping has been improved in the Logar Valley area. Satellite image processing techniques are used to process a subset image of Landsat 8 OLI data (153/36 path/row) including the false color composites (FCC), principal components analysis (PCA) and band-rationing. The results obtained have proven that by using color composite ratio and two-band ration techniques (R:6/7, G:4/2, R:5/4) and (R:4/2, G:6/7, R:5) images with or without supervised classification, is the best method for mapping the rock units. It has also been proven in [16] that better contrast of the rock units in Logar Valley area can be achieved by using FCC technique. The same approach to detect the potential hosts for platinum group and chromite minerals is possible to be applied to other area in the east and southeast of Afghanistan.

3.4 Hydrology

Landsat 8 allows the observation of hydrological state variables such as land surface temperature, surface soil moisture and snow cover over large areas. Numerous researches have been done in hydrological aspect, among them is by Fahnestock et al. [17] to map ice flow in both outlet glaciers and inland tributaries in Greenland, Antarctica, and Southern Alaska. Fahnestock et al. utilize high radiometric sensitivity of the Landsat 8 OLI images to map the ice flow to detect possible similar locations by comparing features in one panchromatic image with the second panchromatic image with a time separation between 16 to 64 days supposing that the surface features would be modified over longer separations. A normalized cross-correlation surface will be generated to determine the best match. Determination of feature offset is then done via mathematical interpolation using PyCorr software. With PyCorr, a processing system that allows velocity mapping of coastal to interior ice sheet with unprecedented temporal coverage is developed by utilizing the advantages of Landsat 8's radiometric resolution, geolocation accuracy, and acquisition rates.

On the other hand, at Colorado River Basin, Senay et al. [18] utilize Landsat 8 to evaluate evapotranspiration map for water planners and managers to understand the water use and water availability. In a supply and demand area especially with the spatiotemporal dynamics of sources including reservoirs and streams requires an efficient water management principle. Since the prediction of actual water used by irrigation vary according to the type of crops in a different location or season, Senay et al. predicted not only the water available at the river basin, but also the water used by crops at a country level. To compute land surface temperature, 528 Landsat 8 images with cloud cover less than 60% were chosen with thermal band 10 while red and NIR bands are used to compute NDVI. The computation of evapotranspiration and other ancillary data was done using Operational Simplified Surface Energy Balance model. The results are then validated using eddy covariance data and compared with water balance-based ET where they show good agreements with each other.

The lake extent for lake inventory and interpretation of long-term changes throughout lake stable seasons is mapped using Landsat 8 by Sheng et al. [19] in mainland Oceania. As Oceania contains various climate zone, the lake stable season in Oceania varies from one area to the other. Hence, to select images based on a season defined using climatic and hydrological variables, LakeTime algorithm is used. Circa-2015 lake map is then produced by selecting images that are captured during lake stable season with low cloud coverage. Lakes are identified using NIR band as well as Band 4, 5 and 7 of OLI. By segmenting the entire NDWI images, the enhancement of water feature and noise-reduction can be achieved using a loose initial threshold. A lake layer is produced in vector GIS format by an automated lake approach for each image. The results are then compared with Circa-2000 map obtained from Landsat 7 and it shows that NDWI images derived from Landsat 8 has less noise compared to Landsat 7. Besides, Landsat 8 has accurate geo referencing as compared to the previous Landsat due to the improved geometric fidelity. To conclude, Sheng et al. has successfully map salt water and fresh water lakes in Oceania.

3.5 Coastal Resources

The spectroradiometric sensitivity of Landsat 8's OLI makes it able to be used in monitoring water quality in coastal wetlands. Therefore, Dube et al. [20] have utilized the OLI/TIRS sensor to detect and map water hyacinth invasive species in Lake Chivero, Zimbabwe. First of all, the digital number format images from Landsat 8 are converted to spectral reflectance by implementing it in a GIS environment. Then, they are corrected using ENVI software and GCP. Analysis of variance and discriminant analysis were used to identify water hyacinth from other land cover and to determine the age groups that the water hyacinth belong to. This study categorized three age groups of water hyacinth namely old, intermediate and young. The results obtained via Landsat 8 was then compared with Landsat 7 and it shows that unlike Landsat 7, Landsat 8 is able to differentiate between other land cover and water hyacinth with impressive accuracy of 92%. Landsat 8 is also able to differentiate the age group with accuracy of 72%. The

study concludes that Landsat 8 provides better dataset for massive mapping of water hyacinth in resource constrained area as compared to Landsat 7.

Other than water hyacinth, Landsat 8 has also been used to detect coral reefs habitat in Red Sea, Egypt by Askary et al. [21]. Close inspection on coral reefs need to be done as they suffer major deterioration, be it due to nature or manmade impacts. Hence in this study, three different images from Landsat 5 (1987), 7 (2000), and 8 (2013) are used to analyze the change in the reef for over 26 years. The image analysis and processing are done via ENVI and ERDAS software. Visible bands are used as they have lower water columns absorption and they are able to identify water-land interface. The water body is further differentiated from coral reef using masks. Misclassification between marine habitats is then done using water column correction followed by change detection analysis to analyze the same scene throughout the years. The results highlighted before the year 2000, indicates an increment in micro algae and seagrass but a reduction in sand intertidal, coral, and sand subtidal. After the year 2000, an increment in sand subtidal and macro-algae is observed with reduction in sand intertidal, coral, and seagrass classes.

Landsat 8 has also been used by Rapinel et al. [22] to map fine-grained plant communities along French Atlantic coastal marshlands. The issue of Landsat 8's resolution that serves as a challenge in mapping heterogeneous habitats has been resolved in [22] by combining fine-grained vegetation units that constitute repetitive combinations at a higher hierarchical level.

Geosymphytosociological method is used to accumulate combinations of four plant communities by mapping fine-grained and heterogeneous vegetation. The satellite images were first orthorectified as well as calibrated radiometrically and atmospherically. Digital Terrain Model (DTM) was then used to outline the marshlands based on topographic and coastline distance criteria. Marshlands then are characterized using all the multispectral bands. This study obtained as high as 89.5% overall accuracy in the coastal marshlands mapping.

3.6 Environmental Monitoring

Monitoring the environment is crucial to assess the quality of our environment for further decision making by federal government or other agencies. Remote sensing has been used for environmental monitoring worldwide, and among one important purpose is to detect biomass burning related fire. In [23], Schroeder et al. have presented an active fire detection algorithm that is applied to the Advanced Spaceborne Thermal Emission and Reflection Radiometer (ASTER) and Landsat-7 ETM+ NIR and SWIR data. A contextual approach with a two-channel fixed threshold are used to explore the SWIR differential radiometric responses. The classification of the fire-affected pixels is done using NIR data. The fire detection algorithm implemented in Landsat 8 is categorized into day and nighttime module which is driven by SWIR fire-sensitive channel 7 data. For daytime, NIR channel 5 data is used to separate emissive fire component with the reflected solar component. However, for night time, the SWIR band is used since it is responsive to the radiance from active fire due to the absence of a reflected solar component. The results show a good quality of fire detection for both day and nighttime imagery.

4. Possible Applications of Landsat 8 Data for Power Utility Companies

Satellite imagery has been a powerful tool in many businesses and has also been implemented in power related applications such as to project future electric demand and to choose power corridors. However due to its major limitation which is the resolution, Landsat 8 has not been fully utilized by the power utility companies. Although the usage of Landsat 8 for power utility companies are limited, there are still several applications that can be done with the data. For an instance, one of the previous successful applications of Landsat 8 is to evaluate evapotranspiration map in river basin. Water in hydroelectric dam evaporates and percolates into the soil. Hence, it is crucial to monitor the evapotranspiration rate to ensure sustainability of the dam. Landsat 7 [24] imagery data has been previously utilized to excerpt the water surface areas of Roseires reservoir, Sudan and Lake Nasser reservoir, Egypt. However, there is yet a study on estimation discharges from reservoir using Landsat 8 data.

As Landsat 8 has also been used for fire detection, it can also be used to monitor forest fire. Transmission line is normally placed in areas that are prone to have bushfire. Power grid may be further interrupted when fire or electric discharge is emitted to the atmosphere due to bushfire. As a result, Landsat 8 is very crucial to monitor and observe the bushfire situation within the transmission line surrounding the area.

Besides, Landsat 8 can also be used for transmission line routing. Routes for new transmission lines are developed by determining proposed substations or end points for a new transmission line. A large geographic area needs to be studied to identify potential corridors, and the most cost savvy and time-consuming solution for this is by using satellite imagery. Landsat 8 data has yet to be used in the selection of transmission line routing, hence this can be a possible applications of Landsat 8 data.

5. Conclusion

Landsat 8 satellite data has been an inexpensive method for forestry, geology and hydrology. To the best of our knowledge, this is the only paper that has provided a detailed review on applications of Landsat-8 data in numerous areas**.** The review proves that Landsat 8 data is suitable to be used for many applications despites of its resolution. There is yet a research of implementing Landsat 8 data for power utility companies, hence this paper has also listed down possible areas that can be looked at for power related areas using Landsat 8. With the availability of Landsat 8 for more years to come, this paper provides insight for researchers to utilize the data better for their research.

Acknowledgement

The author gratefully acknowledged the support and funding of TNB Seed Fund U-TI-RD-18-07 and U-TS-CR-17-01.

References

[1] USGS, "Landsat Missions: Imaging the Earth Since 1972". available online: https://landsat.usgs.gov/landsat-missions-timeline, last visit: July 2018.

[2] Z. Sun, P. Leinenkugel, H. Guo, C. Huang, and C. Kuenzer (2017), "Extracting distribution and expansion of rubber plantations from Landsat imagery using the C5.0 decision tree method," Journal of Applied Remote Sensing, vol. 11, 21.

[3] R. Kafadar and L. Genc (2015), "Determination of Potential Agricultural Lands Using Landsat 8 OLI Images and GIS: Case Study of Gokceada (Imroz) Turkey," World Academy of Science, Engineering and Technology, International Journal of Environmental, Chemical, Ecological, Geological and Geophysical Engineering, vol. 9, 906-909.

[4] Hasituya, Z. Chen, L. Wang, W. Wu, Z. Jiang, and H. Li (2016), "Monitoring Plastic-Mulched Farmland by Landsat-8 OLI Imagery Using Spectral and Textural Features," Remote Sensing, vol. 8, 353.

[5] A. Kavvadias, E. Psomiadis, M. Chanioti, E. Gala, and S. Michas, "Precision Agriculture-Comparison and Evaluation of Innovative Very High Resolution (UAV) and LandSat Data," in HAICTA, 2015, 376-386,

[6] M. Karlson, M. Ostwald, H. Reese, J. Sanou, B. Tankoano, and E. Mattsson (2015), "Mapping Tree Canopy Cover and Aboveground Biomass in Sudano-Sahelian Woodlands Using Landsat 8 and Random Forest," Remote Sensing, vol. 7, 10017.

[7] A. Šimić Milas, P. Rupasinghe, I. Balenović, and P. Grosevski (2015), "Assessment of forest damage in Croatia using Landsat-8 OLI Images," South-east European forestry, vol. 6, 159-169.
[8] F. Ramdani, S. Rahman, and P. Setiani (2015), "Inexpensive method to assess mangroves forest through the use of open source software and data available freely in public domain," Journal of Geographic Information System, vol. 7, 43.
[9] T. Hu, J. Yang, X. Li, and P. Gong (2016), "Mapping urban land use by using landsat images and open social data," Remote Sensing, vol. 8, 151.
[10] S. S. Bhatti and N. K. Tripathi (2014), "Built-up area extraction using Landsat 8 OLI imagery," GIScience & remote sensing, vol. 51, 445-467.
[11] Y. Gu and B. K. Wylie (2015/12/15/ 2015), "Developing a 30-m grassland productivity estimation map for central Nebraska using 250-m MODIS and 30-m Landsat-8 observations," Remote Sensing of Environment, vol. 171, 291-298.
[12] X. Meng and J. Cheng (2018), "Evaluating Eight Global Reanalysis Products for Atmospheric Correction of Thermal Infrared Sensor—Application to Landsat 8 TIRS10 Data," Remote Sensing, vol. 10, 474.
[13] D. J. Amusuk, M. Hashim, A. B. Pour, and S. I. Musa (2016), "Utilization of LANDSAT-8 Data for Lithological Mapping of Basement Rocks of Plateau State North Central Nigeria," The International Archives of Photogrammetry, Remote Sensing and Spatial Information Sciences, vol. 42, 335.
[14] K. Zeinelabedin and A. H. H. El Nadi (2014), "The use of Landsat 8 OLI image for the delination of gossanic ridges in the Red Sea Hills of NE Sudan," Am. J. Earth Sci, vol. 1, 62-67.
[15] J. He, J. Harris, M. Sawada, and P. Behnia (2015), "A comparison of classification algorithms using Landsat-7 and Landsat-8 data for mapping lithology in Canada's Arctic," International Journal of Remote Sensing, vol. 36, 2252-2276.
[16] R. Abdelaziz, Y. Abd El-Rahman, and S. Wilhelm (03 2018), "Landsat-8 data for chromite prospecting in the Logar Massif, Afghanistan," Heliyon, vol. 4, e00542.
[17] M. Fahnestock, T. Scambos, T. Moon, A. Gardner, T. Haran, and M. Klinger (2016/11/01/ 2016), "Rapid large-area mapping of ice flow using Landsat 8," Remote Sensing of Environment, vol. 185, 84-94.
[18] G. B. Senay, M. Friedrichs, R. K. Singh, and N. M. Velpuri (2016/11/01/ 2016), "Evaluating Landsat 8 evapotranspiration for water use mapping in the Colorado River Basin," Remote Sensing of Environment, vol. 185, 171-185.
[19] Y. Sheng, C. Song, J. Wang, E. A. Lyons, B. R. Knox, J. S. Cox, et al. (2016/11/01/ 2016), "Representative lake water extent mapping at continental scales using multi-temporal Landsat-8 imagery," Remote Sensing of Environment, vol. 185, 129-141.
[20] T. Dube, O. Mutanga, M. Sibanda, V. Bangamwabo, and C. Shoko (2017/08/01/ 2017), "Evaluating the performance of the newly-launched Landsat 8 sensor in detecting and mapping the spatial configuration of water hyacinth (Eichhornia crassipes) in inland lakes, Zimbabwe," Physics and Chemistry of the Earth, Parts A/B/C, vol. 100, 101-111.
[21] H. El-Askary, S. H. Abd El-Mawla, J. Li, M. M. El-Hattab, and M. El-Raey (2014/03/19 2014), "Change detection of coral reef habitat using Landsat-5 TM, Landsat 7 ETM+ and Landsat 8 OLI data in the Red Sea (Hurghada, Egypt)," International Journal of Remote Sensing, vol. 35, 2327-2346.
[22] S. Rapinel, J.-B. Bouzillé, J. Oszwald, and A. Bonis (December 01 2015), "Use of bi-Seasonal Landsat-8 Imagery for Mapping Marshland Plant Community Combinations at the Regional Scale," Wetlands, vol. 35, 1043-1054.
[23] W. Schroeder, P. Oliva, L. Giglio, B. Quayle, E. Lorenz, and F. Morelli (2016/11/01/ 2016), "Active fire detection using Landsat-8/OLI data," Remote Sensing of Environment, vol. 185, 210-220.
[24] E. Muala, Y. Mohamed, Z. Duan, and P. van der Zaag (2014), "Estimation of Reservoir Discharges from Lake Nasser and Roseires Reservoir in the Nile Basin Using Satellite Altimetry and Imagery Data," Remote Sensing, vol. 6, 7522.